Particle-size effects on the terahertz transmittance of metallic particle ensembles: Comparison with effective medium theory

Y. Zheng, A. Johnson, E. Pyde, and K. J. Chau[a)]
School of Engineering, University of British Columbia, Okanagan, British Columbia V1V1V7, Canada

(Received 14 December 2009; accepted 26 April 2010; published online 25 May 2010)

We investigate the transmittance of fixed-length ensembles of spherical particles having average radii ranging over two orders of magnitude. The transmittance is interrogated at discrete frequencies in the terahertz regime where the particle radius is subwavelength by at least an order of magnitude. A nonmonotonic dependence of the transmittance on particle radius is observed. As a function of increasing particle size, the transmittance increases to a peak value and then decreases toward zero. Calculations of the complex effective permittivity of the ensemble yield predicted transmittance curves that accurately describe the transmittance decrease as a function of increasing particle size. © *2010 American Institute of Physics*. [doi:10.1063/1.3430547]

Recently, there has been intense research interest in the electromagnetic properties of subwavelength scale metallic particles for applications in sensing,[1] wave-guiding,[2–4] and metamaterials.[5] Metallic particles having lateral dimensions much smaller than the free-space wavelength, λ_0, are unique because they possess a dipolar polarizability dependent on the geometrical features of the medium. An incident electromagnetic wave can induce charge accumulation at the lateral edges of the particle. This dipolar polarizability is absent for normal-incidence illumination of bulk metals having lateral dimensions $\gg \lambda_0$.

Illumination of a subwavelength metallic particle results in an oscillating dipole whose forward and backward radiation characteristics strongly depend the size, shape, and orientation of the metallic particle.[6] Forward electromagnetic wave propagation through collections of subwavelength-sized metallic particles has been recently demonstrated in the terahertz (THz) regime.[7] Millimeter-thick ensembles of subwavelength-sized, micron-scale particles of varying metal type, particle shape, packing density, and particle size have been shown to transmit electromagnetic pulses in the frequency range from 0.01 to 1 THz.[8,9] The mechanism proposed to underlie the transmission phenomenon is dipole-coupling between nearest-neighbor particles.

In this letter, we quantitatively characterize the particle-size dependence of electromagnetic wave propagation through metallic spherical particle ensembles. Linearly polarized, single-cycle THz pulses with frequency components spanning from 0.01 to 1.0 THz are directed at normal incidence onto a sample cell (composed of THz-transparent polystyrene front and back walls) housing a dense ensembles of copper spheres. The independent variable is the radius of the spheres; spheres with nominal mean radii of 5 ± 2 μm, 43 ± 5 μm, 97 ± 5 μm, 125 ± 5 μm, 141 ± 4 μm, 186 ± 9 μm, 231 ± 9 μm, 280 ± 8 μm, and 335 ± 15 μm are employed. Control variables include the thickness of the sample cell ($L = 3.0 \pm 0.1$ mm), the volume fraction of metal in the metal-air ensemble ($f = 0.55 \pm 0.05$), the shape of the particles (spherical), and the type of metal (copper). The dependent variables are the transmittance of the ensemble and the transmission polarization, which is measured by sampling the angular distribution of the THz electric field amplitude in the plane normal to the propagation direction.[9,10]

THz time-domain spectroscopy is employed to measure the real part of the electric field $E_t'(t)$ of THz pulses transmitted through metallic particle ensembles. The imaginary component of the electric field $E_t''(t)$ is obtained by Hilbert transformation of $E_t'(t)$. Fourier transformation of the complex time-dependent electric field $\underline{E}_t(t) = E_t'(t) + iE_t''(t)$ yields the complex frequency-dependent electric field $\underline{E}_t(\omega)$, from which the transmission intensity spectrum is given by $I_t(\omega) = (1/2)\epsilon_0 \underline{E}_t(\omega)\underline{E}_t^*(\omega)$, where ϵ_0 is the free-space permittivity and $\underline{E}_t^*(\omega)$ is the complex conjugate of the transmitted electric field. The transmittance of the ensemble is given by $T(\omega) = I_t(\omega)/I_i(\omega)$, where $I_i(\omega)$ is the intensity spectrum of the incident THz pulse (corresponding to the THz pulse transmitted through the empty polystyrene sample cell).

Figure 1 displays $T(\omega)$ for 3-mm-thick ensembles where a ranges from 5 to 231 μm (ensembles of 280-μm-radius

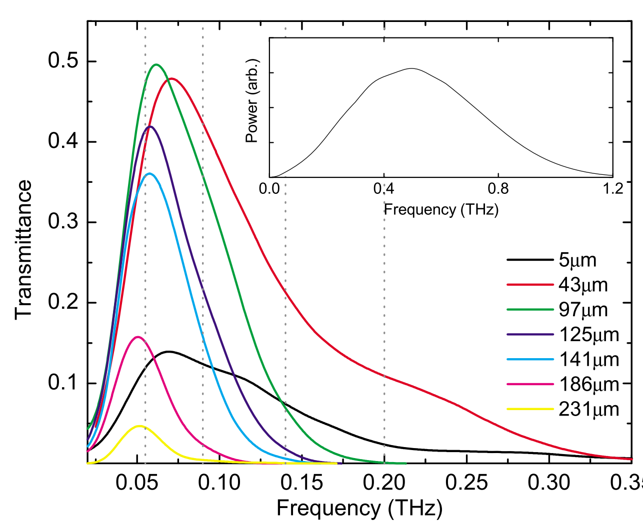

FIG. 1. (Color online) Transmittance of the ensembles for mean particle radius ranging from 5 to 231 μm. The dashed vertical lines on the graph indicate the frequency values for which the transmittance will be studied as a function of particle size. The inset depicts the power spectrum of the incident pulse.

a)Electronic mail: kenneth.chau@ubc.ca.

 © 2010 American Institute of Physics

Downloaded 31 May 2010 to 129.8.242.67. Redistribution subject to AIP license or copyright; see http://apl.aip.org/apl/copyright.jsp

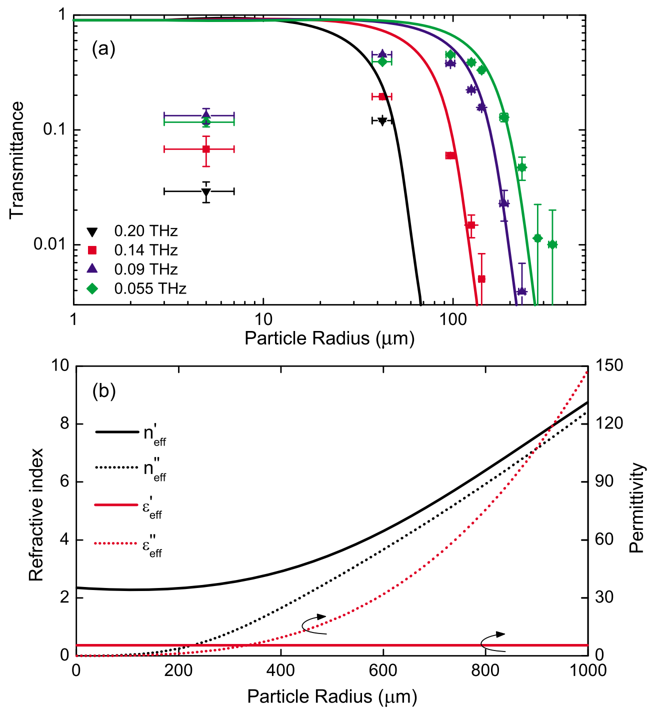

FIG. 2. (Color online) (a) Log-log plot of the measured transmittance of the ensemble at 0.20 THz (inverted triangles), 0.14 THz (squares), 0.09 THz (upright triangles), and 0.055 THz (diamonds) as a function of the mean particle radius. Measurements at each value of particle radius are obtained from the average of at least three independent measurements. The solid lines (as they appear in the figure from left to right) are the predicted transmittance curves calculated at 0.20 THz, 0.14 THz, 0.09 THz, and 0.055 THz using Eq. (4) with a volume fraction $f=0.55$ matching the experimental conditions. (b) Depicts the real (solid line) and imaginary (dotted line) parts of the complex effective refractive index (left vertical axis) and the complex effective permittivity (right vertical axis) of the ensemble at 0.055 THz.

and 335-μm-radius particles exhibit nearly no transmission and are not plotted). It is notable that the ensembles are partially transparent only in the low-frequency range spanning from 0.01 to 0.3 THz. As a increases from 5 to 231 μm, the peak transmittance shifts from 0.08 to 0.05 THz, corresponding to an equivalent shift in the peak free-space wavelength, λ_p, from 3.7 to 6.0 mm. For the 5-μm-radius particle ensemble, $a/\lambda_p \simeq 0.001$; for the 231-μm-radius particle ensemble, $a/\lambda_p \simeq 0.039$. The full-width-at-half-maximum of the transmittance decreases from 0.10 to 0.03 THz as a increases from 5 to 231 μm. Reduction in the spectral width with increasing a is characterized by a preferential reduction in the transmittance at higher frequencies.

We quantify the particle-size dependence of the transmittance at four discrete frequencies (0.055, 0.09, 0.14, and 0.20 THz) spanning the range of the transmittance curves in Fig. 1. As shown in Fig. 2(a), the transmittance exhibits a non-monotonic dependence on the particle radius. Significant (high-signal-to-noise) transmittance values at 0.055 THz are measured for all the ensembles depicted in Fig. 1. The transmittance values at 0.055 THz rise as a increases from 5 to 43 μm and then drop sharply for $a>97$ μm. Peak transmittance is observed for $a/\lambda_0 \simeq 0.018$. Similar trends are observed at 0.09, 0.14, and 0.20 THz, where the transmittances rise as a increases from 5 to 43 μm and then drop for $a>43$ μm.

We derive the complex effective permittivity of the particle ensemble by considering a scattering medium containing a collection of metallic spheres immersed in a surrounding medium of unity permittivity. The metallic spheres have complex permittivity $\underline{\epsilon}_m = \epsilon'_m + i\epsilon''_m$ and occupy a volume fraction f. For spheres with radius $a \ll \lambda_0$, the real part of the effective permittivity can be approximated by a volumetric average of the real part of the permittivities of the constituents[11]

$$\epsilon'_{\mathrm{eff}} = \frac{1+2f(\epsilon'_m-1)/(\epsilon'_m+2)}{1-f(\epsilon'_m-1)/(\epsilon'_m+2)}. \tag{1}$$

Electromagnetic losses due to scattering from the spheres are described by an imaginary part of the effective permittivity $\epsilon''_{\mathrm{eff}}$, which is derived by considering the total power loss due to Rayleigh scattering from an isolated spherical particle immersed in a homogeneous dielectric medium of real effective refractive index $n'_{\mathrm{eff}} \simeq \sqrt{\epsilon'_{\mathrm{eff}}}$. Under the condition of independent scattering (where mutual interactions between two or more spherical particles can be neglected), the imaginary part of the effective permittivity of the ensemble is given by[11]

$$\epsilon''_{\mathrm{eff}} = 2fk_{\mathrm{eff}}^3 a^3 \left| \frac{(\underline{\epsilon}_m-1)/(\underline{\epsilon}_m+2)}{1-f(\underline{\epsilon}_m-1)/(\underline{\epsilon}_m+2)} \right|^2, \tag{2}$$

where $k_{\mathrm{eff}} = k_0 n'_{\mathrm{eff}} \simeq k_0\sqrt{\epsilon'_{\mathrm{eff}}}$ is the real part of the effective wave vector in the medium surrounding the particle. At THz frequencies where $|\epsilon'_m| \gg 1$ and $|\underline{\epsilon}_m| \gg 1$, the complex effective permittivity of the ensemble $\underline{\epsilon}_{\mathrm{eff}} = \epsilon'_{\mathrm{eff}} + i\epsilon''_{\mathrm{eff}}$ is independent of $\underline{\epsilon}_m$ and can be expressed as

$$\underline{\epsilon}_{\mathrm{eff}} = \frac{1+2f}{1-f} + i2fk_{\mathrm{eff}}^3 a^3 \left| \frac{1}{1-f} \right|^2. \tag{3}$$

For a flat slab of material with thickness L and complex effective refractive index $\underline{n}_{\mathrm{eff}} = \sqrt{\underline{\epsilon}_{\mathrm{eff}}}$ immersed in free-space, the transmittance for normal incidence illumination is[12]

$$T = \frac{t^2 e^{-\alpha L}}{1-r^2 e^{-2\alpha L}}, \tag{4}$$

where $r = |(\underline{n}_{\mathrm{eff}}-1)/(\underline{n}_{\mathrm{eff}}+1)|^2$ and $t = 4\underline{n}_{\mathrm{eff}}/|\underline{n}_{\mathrm{eff}}+1|^2$ are the respective reflectance and transmittance of the air/slab interface and $\alpha = 2k_0 n''_{\mathrm{eff}}$ is the intensity attenuation coefficient in the effective medium.

Figure 2(a) plots the predicted transmittance curves of a $L=3$ mm thick ensemble of particles described by a complex permittivity $\underline{\epsilon}_{\mathrm{eff}}$ derived at 0.055, 0.09, 0.14, and 0.20 THz. In the limit where a approaches zero, the predicted transmittances at all frequencies approach 0.72. The theory predicts a frequency-dependent monotonic decrease in the transmittance as a function of particle radius; the curves for T(0.055 THz), T(0.09 THz), T(0.14 THz), and T(0.20 THz) are less than 0.001, respectively, for $a>300$ μm, $a>200$ μm, $a>120$ μm, and $a>70$ μm. Good agreement between the theory and experiment is observed for T(0.055 THz) in the range $a>141$ μm, for T(0.09 THz) in the range $a>125$ μm, and for T(0.14 THz) in the range $a>97$ μm. The predicted transmittance and experimental measurement match in the region where the transmittance decreases as a function of increasing particle radius and departs in the region where the transmittance increases as a function of increasing particle size. The region

Downloaded 31 May 2010 to 129.8.242.67. Redistribution subject to AIP license or copyright; see http://apl.aip.org/apl/copyright.jsp

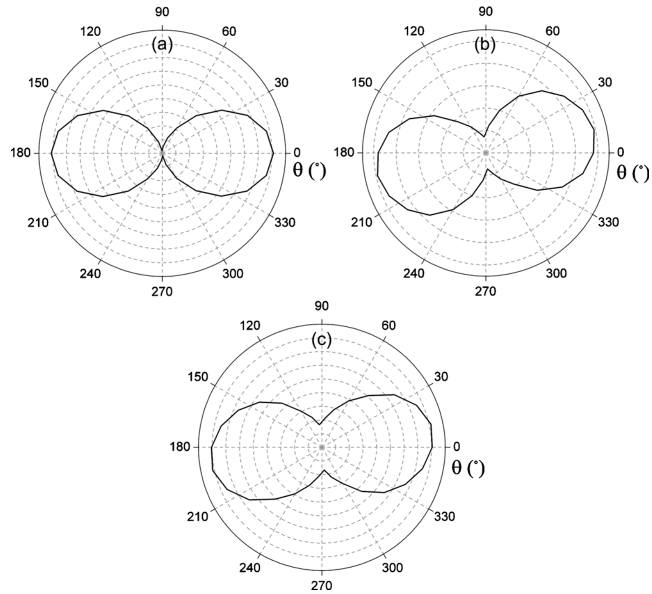

FIG. 3. Polar plot of the angular distribution of the electric field amplitude of the transmitted pulse through (a) the empty sample cell, (b) the 43-μm-radius particle ensemble, and (c) the 186-μm-radius particle ensemble. The angular distribution of the electric field amplitude in each plot corresponds to the average of at least three independent measurements.

of mismatch occurs for smaller particle sizes in which the number density and surface-area-to-volume ratio are both high. The former leads to increased mutual interactions between particles (undermining the independent scattering assumption used to derive $\epsilon''_{\mathrm{eff}}$), and the latter leads to increased Ohmic dissipation within the skin depth of the particles.

The real and imaginary parts of the effective permittivity and refractive index as a function of a are plotted in Fig. 2(b) at a frequency of 0.055 THz. For all values of a, $\epsilon'_{\mathrm{eff}}=5$. On the other hand, $\epsilon''_{\mathrm{eff}}$ increases from $\simeq 0$ to $\simeq 147$ as a increases from 0 to 1000 μm. The a-dependence of both n'_{eff} and n''_{eff} are caused by the monotonic increase in $\epsilon''_{\mathrm{eff}}$ as a function of a.

Figure 3 illustrates polar plots of the angular distribution of the amplitude of the incident electric field, along with that of the amplitude of the transmitted electric field through particles with mean radii of 43 and 186 μm. The polarization of the transmission through the 43-μm-radius particles is slightly depolarized relative to that of the incident electric field, evidenced by an increased electric field amplitude in the direction orthogonal to the incident polarization. Greater depolarization of the transmission through the ensemble of 186-μm-radius particles indicates increased out-of-plane scattering with increasing particle size. Relative to the 43-μm-radius particles, the transmission through 186-μm-radius particles is mediated to a greater extent by multiply-scattered radiation escaping from the back of the sample with randomly oriented polarization.

In conclusion, the transmittance of dense, fixed-length ensembles of metallic particles with mean radius varying over two orders of magnitude has been studied in the range from 0.01 to 0.3 THz. Transmittance curves predicted from the application of effective medium theory accurately describe the behavior of the measured transmittance for larger particle sizes. For smaller particle sizes, discrepancies between the theory and experiment are attributed to the effect of mutual scattering between particles and Ohmic dissipation in the skin depth of the particle.

The authors thank an anonymous referee for helpful suggestions that have greatly improved the manuscript clarity. K.J.C. acknowledges A. Y. Elezzabi for helpful discussions and his guidance. This work was supported by the Natural Sciences and Engineering Research Council (NSERC) of Canada.

[1]A. D. McFarland and R. P. Van Duyne, Nano Lett. **3**, 1057 (2003).
[2]M. Quinten, A. Leitner, J. R. Krenn, and F. R. Aussenegg, Opt. Lett. **23**, 1331 (1998).
[3]S. A. Maier, P. G. Kik, H. A. Atwater, S. Meltzer, E. Harel, B. E. Koel, and A. A. G. Requicha, Nat. Mater. **2**, 229 (2003).
[4]K. Wang and D. M. Mittleman, Nature (London) **432**, 376 (2004).
[5]N. Engheta, Science **317**, 1698 (2007).
[6]K. L. Kelly, E. Coronado, L. L. Zhao, and G. C. Schatz, J. Phys. Chem. B **107**, 668 (2003).
[7]K. J. Chau, G. D. Dice, and A. Y. Elezzabi, Phys. Rev. Lett. **94**, 173904 (2005).
[8]K. J. Chau and A. Y. Elezzabi, Phys. Rev. B **73**, 085419 (2006).
[9]K. J. Chau and A. Y. Elezzabi, Phys. Rev. B **72**, 075110 (2005).
[10]N. C. J. van der Valk, A. M. van der Marel, and P. C. M. Planken, Opt. Lett. **30**, 2802 (2005).
[11]J. A. Kong, *Electromagnetic Wave Theory* (Wiley, New York, 1986).
[12]E. Nichelatti, J. Opt. A, Pure Appl. Opt. **4**, 400 (2002).

Downloaded 31 May 2010 to 129.8.242.67. Redistribution subject to AIP license or copyright; see http://apl.aip.org/apl/copyright.jsp